ISSN: 2687-8100

Archives in Biomedical Engineering & Biotechnology

DOI: 10.33552/ABEB.2024.07.000672

Iris Publishers

Research Article

Synthetic Pyrazolone Derivatives as Novel Antiviral Drug Leads Against Chikungunya Virus: *In Vitro* and *In Silico* Evaluations

Tiago Barbosa Soares[1], Luciene Soares Silva[1], Vitor Won-Held Rabelo[1], Leonardo dos Santos Corrêa Amorim[1,2], Maria Leonisa Sanchez Nuñez[1], Carolina Oliveira da Silva[1], Percilene Fazolin Vegi[3], Paula Alvarez Abreu[4], Alice Maria Rolim Bernardino[3], Claudio Cesar Cirne dos Santos[1] and Izabel Christina Nunes de Palmer Paixão[1,5,6]*

[1]*Programa de Pós-graduação em Ciências e Biotecnologia, Instituto de Biologia, Universidade Federal Fluminense, Niterói, RJ, Brazil*

[2]*Gerência de Desenvolvimento Tecnológico, Instituto Vital Brazil, Niterói, RJ , Brazil*

[3]*Programa de Pós-graduação em Química, Instituto de Química, Universidade Federal Fluminense, Niterói, RJ, CEP 24020-007, Brazil*

[4]*Instituto de Biodiversidade e Sustentabilidade (NUPEM), Universidade Federal do Rio de Janeiro, Macaé, RJ, Brazil*

[5]*Departamento de Biologia Celular e Molecular, Instituto de Biologia, Universidade Federal Fluminense, Niterói, RJ, Brazil*

[6]*Programa de Pós-graduação em Biotecnologia Marinha e Neurologia/Neurociências, Universidade Federal Fluminense, Niterói, RJ, Brazil*

***Corresponding author:** Izabel Christina Nunes de Palmer Paixão, Departamento de Biologia Celular e Molecular, Instituto de Biologia, Universidade Federal Fluminense, Niterói, RJ, CEP 24210-201, Brazil

Received Date: May 31, 2024

Published Date: July 17, 2024

Abstract

Chikungunya virus (CHIKV) is an arthropod-borne pathogen responsible for Chikungunya fever, a neglected tropical disease of global health concern. Despite the low mortality rates, this illness can persist for months or even years after acute infection, causing debilitating arthritis and serious economic outcomes. Currently, the lack of licensed vaccines or antiviral drugs limits disease control which emphasizes the critical need to develop new therapies. Herein, the antiviral potential of nine pyrazolone derivatives was evaluated against CHIKV replication by using *in vitro* and *in silico* methods. Among the compounds, three derivatives (**1a, 1b, and 1i**) showed the highest antiviral activity against CHIKV replication at 50 µM. Compound **1b** showed an EC_{50} of 26.44 µM, followed by compounds **1b and 1i** with EC_{50} values of 34.67 µM and 46.36 µM, respectively. In addition, these compounds exhibited good selectivity with selectivity indexes of 39.02 **(1a), 55.67 (1b), and 21.13 (1i)**. Our SAR studies revealed some stereo electronic properties that are likely essential to their antiviral activity. Further, we investigated the mechanism of action of the most active compounds. Interestingly, the three compounds showed virucidal activity and inhibited early steps of virus replication. Compound **1b** also impaired virus replication at later post-entry steps, suggesting that these derivatives may act at different targets. Pharmacokinetic, and toxicological predictions reinforced the safety and drug-like profiles of these derivatives. Therefore, this is the first report of the anti-CHIKV activity of pyrazolone derivatives, and our data point to them as promising leads for antiviral drug discovery to combat CHIKV infections.

Keywords: Chikungunya; Pyrazolone; Antiviral; Drug discovery

Abbreviations

CC_{50}: concentration required to decrease cell viability by 50%; $_{ele}$: electrostatic charge of the C_4 carbon atom of the phenyl group; CHIKV: Chikungunya virus; CQ: chloroquine; DM: dipole moment; DMEM: Dulbecco's Modified Eagle Medium; EC_{50}: concentration required to inhibit virus replication by 50%; E_{HOMO}: energies of the highest occupied molecular orbital; E_{LUMO}: energies of the lowest unoccupied molecular orbital; FBS: fetal bovine serum; HIA: human intestinal absorption; HOMO: highest occupied molecular orbital; Hpi: hours post-infection; LUMO: lowest unoccupied molecular orbital; MC: methylcellulose; MOI: multiplicity of infection; Mpro: main protease; MSA: molecular surface area; MV: molecular volume; MW: molecular weight; nsP: nonstructural protein; Oval: ovality; PSA: polar surface area; SI: selectivity index; VC: virus control.

Introduction

Chikungunya virus (CHIKV) is a mosquito-borne pathogen that belongs to the *Alphavirus* genus and Togaviridae family and, which includes other "old world" alphaviruses [1,2]. CHIKV has a single-strand positive sense RNA with a size of ~12kb. The RNA molecule has two open read frames (ORF) that encode four nonstructural proteins (nsP1-nsP4) and six structural proteins or peptides (E1,E2,E3,C,TF and 6K) [1]. The transmission of this virus occurs through two different cycles, such as a sylvatic cycle, in which transmission occurs in non-human primates, and an urban cycle, where the virus is transmitted to humans by *Aedes aegypti* and *Aedes albopictus* mosquitoes [3-5].

For the past decades, CHIKV has caused several outbreaks in some continents, such as Africa, Asia, and the Americas. Since its outbreak in the Caribbean Islands in 2013, more than three million cases of CHIKV were described worldwide [6]. In 2022, most cases were reported in Brazil followed by India, Paraguay, Guatemala, and Thailand [7]. In this period, Brazil has registered more than 174,000 cases of CHIKV infections which reflects an increase of 78.9% in comparison to 2021 [8]. Recently, this infection was listed as a neglected tropical disease by World Health Organization [9].

CHIKV is the causative agent of Chikungunya fever which is characterized by fever, skin rash, myalgia, and arthralgia [10]. This disease has two different phases: acute and chronic. The acute one is mostly described by fever and arthralgia and lasts for 5-14 days. However, more than 40% of patients evolve to chronic disease where arthritic manifestations can occur, such as chronic inflammatory pain which, in turn, leads to the disability of infected individuals. Also, the chronic phase can persist for months or years and, in addition to the health issues, this disease may cause substantial economic damage to the most affected communities [11]. Usually, the symptoms of CHIKV infection overlap with other arboviral infections, especially due to the high circulation of these viruses simultaneously in the same geographical area, which poses a challenge for disease diagnostics and control [10,12]. Besides, there is no currently available vaccine or specific drugs for the treatment and prevention of CHIKV infections, which makes the development of new drugs urgently needed [5].

In this scenario, heterocyclic molecules play a remarkable role in drug discovery. Among them, pyrazolone derivatives have received attention since 1883 when Knorr first synthesized the antipyretic, analgesic, and anti-inflammatory drug antipyrine [13]. Pyrazolone is a five-membered ring that contains two nitrogen atoms and a ketone function, and two nuclei are more frequently found in bioactive derivatives: 3-pyrazolone and 5-pyrazolone [14]. Several synthetic methods have been described to obtain novel derivatives with great yield and purity, resulting in a highly structural diverse, and versatile scaffold [13,15]. In addition, the pyrazolone core has a noteworthy pharmaceutical importance because it is a bioisostere for some nitrogen-containing heterocycles and has a wide range of biological activities such as antimicrobial, anticancer, anti-inflammatory, antioxidant, and antiviral [16,17]. However, there are no reports on the anti-CHIKV activity of pyrazolone derivatives in the literature to date. Therefore, we report for the first time the evaluation of the antiviral potential of pyrazolone derivatives against CHIKV replication. Further, structure-activity relationship, ADMET, and mechanism of action studies were carried out by combining *in vitro* and *in silico* methods.

Materials and Methods

Cells and viruses

Vero cells (ATCC CCL-81) were grown in Dulbecco's Modified Eagle Medium (DMEM) supplemented with 5% fetal bovine serum (FBS), 100 UI/mL penicillin, 100 µg/mL streptomycin, and 2.5 µg/mL amphotericin B at 37°C under a humidified 5% CO_2 atmosphere. A Brazilian isolate of CHIKV reported previously by our group [18] was used in this work. Virus stock was propagated in Vero cells at a multiplicity of infection (MOI) of 0.1. At 48 hours post-infection (hpi), supernatants were collected, clarified, and stored at -80°C.

Compounds

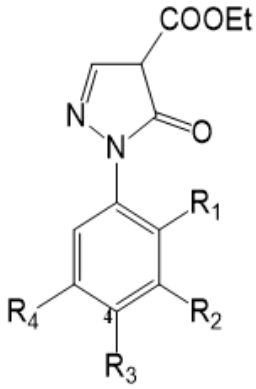

1a: R_1=R_2=R_3=R_4= H
1b: R_1= Cl; R_2= H; R_3= Cl; R_4= H
1c: R_1= H; R_2= Cl; R_3= H; R_4= Cl
1d: R_1= H; R_2=R_3= Cl; R_4= H
1e: R_1=R_2= H; R_3= Cl; R_4= H
1f: R_1= Cl; R_2=R_3=R_4= H
1g: R_1= F; R_2=R_3=R_4= H
1h: R_1=R_2= H; R_3= F; R_4= H
1i: R_1=R_2= H; R_3= OMe; R_4= H

Figure 1: 2D structures of the pyrazolone derivatives evaluated in this work.

Nine pyrazolone derivatives (Figure 1) were obtained as described elsewhere [17,19-21]. All derivatives were dissolved in sterile DMSO, and 50 mM stocks were prepared while chloroquine (CQ; Sigma-Aldrich, Brazil) was prepared in sterile water to a final concentration of 50 mM. All stocks were stored at -20 °C until use.

Cytotoxicity assay

The cytotoxic effects of the compounds were determined using the [(3-(4,5-dimethylthiazol-2-yl)-2,5-diphenyltetrazolium bromide (MTT; Sigma-Aldrich). Briefly, Vero cells were seeded onto a 96-well plate at a density of 10^4 cells per well a day before the experiment and were treated with different concentrations of the compounds (100, 200, 400, and 800 μM) for 72 h at 37 °C and 5% CO_2. Then, the compounds were removed and MTT solution (5 mg/mL) was added and incubated for a further 4 hrs. After this, the MTT solution was removed and DMSO was added to dissolve the formazan crystals under gentle rocking for 20 min at room temperature. Finally, absorbance was measured at 545 nm using the TP-Reader Thermo Plate microplate reader. Three independent assays were carried out in triplicate. Cell viability was calculated relative to untreated cell control and the concentration required to decrease cell viability by 50% (CC_{50}) was estimated by linear regression using GraphPad Prism 6.

Antiviral screening and plaque reduction assay

Vero cells were seeded at 2 x 10^5 cells/well in a 24-well plate overnight at 37 °C under a 5% CO_2 atmosphere. Cells were infected with CHIKV (MOI = 0.001) for 1 hr at 37°C. After virus attachment, virus inoculum was discarded and media containing 50 μM of the compounds was added. At 24 h, cells were lysed by freezing and thawing, supernatants were harvested, and the virus titer was determined using a plaque reduction assay. The experiments were carried out twice in triplicate and the inhibition rates were calculated in comparison to the untreated and infected cell control, namely virus control (VC). CQ (50 μM) was used as a positive control since the *in vitro* anti-CHIKV activity has been described in the literature [22].

For plaque reduction assays, monolayers of Vero cells were infected with 10-fold dilutions of CHIKV suspensions for 1 hr at 37 °C with 5% CO_2. Next, virus inoculum was replaced by media supplemented with 5% FBS and 1.5% methylcellulose (MC), and cells were incubated for 48 hrs at 37°C with 5% CO_2. Finally, cells were fixed and stained with 10% formaldehyde and 0.2% crystal violet and virus titers were determined as PFU/mL.

Determination of the EC_{50} of the most active compounds

The antiviral potency of the most active compounds (**1a**, **1b**, and **1i**) and CQ were also evaluated. For this purpose, Vero cells grown in 24-well plates (2 x 10^5 cells/well) on the day before the experiment were infected with CHIKV at an MOI of 0.001 for 1 h at 37 °C under 5% CO_2. After that, the virus was discarded and cells were treated with different concentrations (3.125, 6.25, 12.5, 25, and 50 μM) for 24 h at 37°C under 5% CO_2. At 24 hpi, cells were lysed by freezing and thawing, and supernatants were collected for plaque assays as abovementioned. Two independent experiments were run in triplicate and inhibition rates were calculated in reference to the untreated and infected cells. The concentration required to inhibit virus replication by 50% (EC_{50}) was calculated from dose-response curves using GraphPad Prism 6.

Virucidal assay

CHIKV suspensions containing approximately 10^4 PFU were treated with 50 μM of the pyrazolone derivatives or CQ for 2 h at 37 °C. After that, virus suspensions were diluted (1:50) and were used to infect confluent monolayers of Vero cells for 1 hr at 37 °C. Then, the virus inoculum was removed, and cells were overlaid with media containing 1.5% MC and 5% FBS. After incubation of 48 hrs at 37 °C under a 5% CO_2 atmosphere, cells were fixed and stained with 10% formaldehyde and 0.2% crystal violet, and the virus titers were determined as PFU/mL. The virucidal activity was determined relative to the untreated virus suspensions. The experiment was performed thrice in triplicate.

Time of addition assay

Vero cells were plated in a 24-well plate at 2 x 10^5 cells/well one day before the experiment. Cells were infected with CHIKV (MOI of 0.001) for 1 hr at 37°C under 5% CO_2. Cells were treated with the pyrazolone derivatives or CQ at 300 μM as suggested elsewhere [23] and different treatment protocols were applied to investigate at which step of virus replication the compounds act. Compounds were added 1 h prior to infection (-1 hpi), during infection (0 hpi), and several times after infection (1,2,4, and 6 hpi). Cells were kept with the compounds for 1 h and then, replaced by media without compounds. At 7 hpi, the media of all wells was discarded, and cells were covered with DMEM supplemented with 5% FBS and 1.5% MC and incubated for 48 h at 37°C under a 5% CO_2 atmosphere. Finally, cells were fixed and stained with 10% formaldehyde and 0.2% crystal violet and the number of PFU was counted. Infection and inhibition rates were calculated in relation to the untreated and infected control. Two independent experiments were carried out in triplicate.

SAR studies

The three-dimensional structures of the pyrazolone derivatives were constructed and optimized using the Spartan´10 program (Wavefunction Inc., Irvine, CA, USA). Initially, structures were submitted to a conformational analysis in vacuum using molecular mechanics and the MMFF force field. The lowest-energy conformer was subjected to a geometry optimization step using the semi-empirical RM1 method, followed by an *ab initio* calculation using the Hartree-Fock method and the 6-31G* basis set. Finally, the following stereo electronic properties of the compounds were calculated: molecular weight (MW), molecular surface area (MSA) and volume (MV), ovality (Oval), polar surface area (PSA), energies of the highest occupied molecular orbital and lowest unoccupied molecular orbital (E_{HOMO} and E_{LUMO}, respectively), dipole moment (DM) as well as the electrostatic charge of the C_4 carbon atom of the phenyl group (C_{ele}). Besides, the molecular electrostatic potential

(MEP) map and the distribution and density maps of HOMO and LUMO were calculated.

Prediction of pharmacokinetic and toxicological properties

The theoretical pharmacokinetic and toxicological properties of the most active compounds (**1a**, **1b**, and **1i**) and CQ were analyzed. The admetSAR 2 server [24] was employed to predict human intestinal absorption (HIA) and carcinogenicity, whereas genotoxicity (based on the AMES test), hepatotoxicity, and cardiotoxicity (based on inhibition of hERG I and II) were predicted using the pkCSM server[25]. Toxic effects on reproductive systems and irritant effects as well as drug-likeness and drug-score parameters were predicted using the Osiris Property Explorer server. Additionally, the compounds were also evaluated according to industry rules, like Lipinski's "rule of five", GSK 4/400, and Pfizer 3/75 using the FAF-Drugs4 webserver [26].

Statistical analysis

Data are expressed as mean ± standard deviation and all analyses were carried out with GraphPad Prism 6.0 (San Diego, CA, USA). Statistical analyses were performed with one-way ANOVA followed by the Tukey test. Statistically significant differences were considered when the p-value < 0.05.

Results

Cytotoxicity and anti-CHIKV evaluation of the pyrazolone derivatives

Initially, the cytotoxic effects of the pyrazolone derivatives were investigated by MTT assay. Incubation of the compounds with Vero cells for 72hrs resulted in low cytotoxicity. Consequently, the CC_{50} values of the derivatives varied from 579 µM (**1h**) to 1,472 µM (**1b**) which are higher than the one observed for the control drug CQ (420 µM) (Table 1). Since the compounds presented low cytotoxicity, we evaluated their antiviral activity against CHIKV replication in Vero cells at a non-toxic concentration (50µM). Among the nine compounds, five derivatives displayed weak antiviral activity with inhibition rates lower than 50% while compound **1e** had moderate activity (virus titer was decreased by 56.87%). By contrast, compounds **1a**, **1b**, and **1i** exhibited stronger inhibitory activity and were able to reduce the virus titer by 68.15%, 78.86%, and 77.92%, respectively. Likewise, CQ had a strong activity with inhibitory activity of 99.52%.

Table 1: Cytotoxicity and antiviral activity against CHIKV of the pyrazolone derivatives and the control drug chloroquine (CQ).

Compound	CC_{50} (µM)[a]	Inhibition (%)[b]	EC_{50} (µM)[c]	SI[d]
1a	1,353 ± 17.02	68.15	34.67 ± 6.94	39.02
1b	1,472 ± 40.42	78.86	26.44 ± 5.80	55.67
1c	694 ± 45.08	21.33	ND	ND
1d	831 ± 39.21	18.67	ND	ND
1e	1,130 ± 6.83	56.87	ND	ND
1f	705 ± 8.17	20.67	ND	ND
1g	1,254 ± 29.37	21.33	ND	ND
1h	579 ± 11.68	47.45	ND	ND
1i	980 ± 18.12	77.92	46.36 ± 6.50	21.13
CQ	420 ± 0.02	99.52	13.27 ± 9.75	31.65

[a]CC_{50}: concentration required to decrease 50% of cell viability; [b]Inhibition rate (%) of CHIKV replication in Vero cells at 50 µM; [c]EC_{50}: concentration required to inhibit virus replication by 50%; [d]Selectivity index (SI) was calculated as the ratio of CC_{50} to $EC_{50;}$ ND: not determined.

Furthermore, the EC_{50} values of the most active derivatives (**1a**, **1b**, and **1i**) were calculated from dose-response curves and compared to CQ (Table 1). All compounds reduced virus titer in a dose-dependent manner and compound **1b** showed the highest activity (EC_{50}= 26.44 µM), followed by compounds **1a** (EC_{50}= 34.67 µM) and **1i** (EC_{50}= 46.36 µM), respectively. Although CQ is, at least, two-fold more potent than the pyrazolone derivatives, compounds **1a** and **1b** exhibited greater selectivity (SI= 39.02 and 55.67, respectively).

SAR evaluation

Since the unsubstituted pyrazolone scaffold was endowed with a promising anti-CHIKV activity, we conducted a SAR analysis to investigate structural features that are important to the antiviral profile of these compounds. The introduction of chlorine atoms at *ortho* and *para* positions of the phenyl group, like the 2,4-dichloro derivative (**1b**) resulted in improved activity. In contrast, the addition of halogens at the *para* position alone (**1e** and **1h**) decreased their activity which, in turn, was even more reduced when these substituents were added to the *ortho* position solely (**1f** and **1g**). Besides, the introduction of *meta* substituents, such as 3,5-dichloro (**1c**) or 3,4-dichloro (**1d**) led to a drastic reduction in their activity. Our findings indicated that the presence of electron-withdrawing groups at the *para* and *ortho* positions of the phenyl ring is likely essential to maintain their antiviral potential. Also, we observed that the introduction of an electron-donating group at the *para* position, like methoxy (**1i**), also yielded a more active compound.

In addition, several stereo electronic descriptors were calculated and correlated to the inhibitory activity of the compounds (Table 2). We did not observe a clear correlation between their biological activity and steric features such as MW, MSA, MV, and ovality. Nonetheless, the PSA parameter seems to have an important contribution to their activity, because the most active compounds **1a** and **1i** presented the highest values (43.70 and 49.62 Å^2, respectively). Regarding the electronic features, we noticed that the activity was moderately correlated to E_{HOMO} and E_{LUMO} values which means that the higher these energies, the higher their inhibitory potential. In general, LUMO orbitals were more concentrated over the carboxyl group (Figure 2). The introduction of chlorine atoms at *ortho* and *para* positions of the phenyl ring (**1b**) or the addition of the *p*-methoxy group in the same ring (**1i**) led to an increased density of these orbitals over the phenyl ring, which might be involved to the interaction with their molecular target. By contrast, no significant differences were observed in the HOMO density and distribution maps, nor the MEP maps (Data not shown).

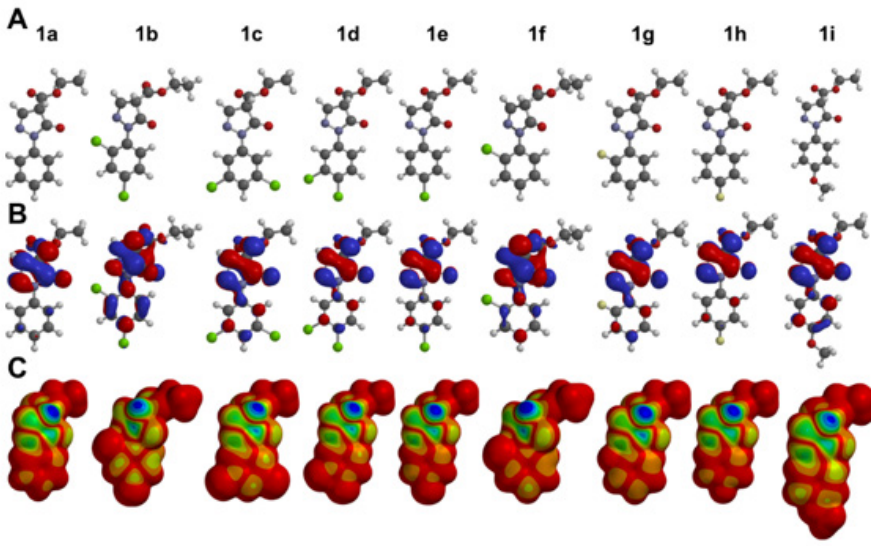

Figure 2: Comparison of stereoelectronic features of the pyrazolone derivatives. A) Lowest-energy conformer; B) LUMO distribution maps; and C) LUMO density maps encoded into a surface of 0.002 e/au3 and generated in the range of 0 to 0.041.

Table 2: Stereo electronic descriptors of the pyrazolone derivatives calculated using the Spartan'10 software.

Compound	MW	MSA	MV	Oval	PSA	E_{HOMO}	E_{LUMO}	DM	C_{ele}
1a	232.24	257.29	233.32	1.40	43.70	-8.16	2.81	2.22	-0.19
1b	301.13	286.45	259.75	1.45	43.43	-8.70	2.62	3.23	0.18
1c	301.13	287.52	260.00	1.46	43.62	-8.75	2.47	4.62	-0.35
1d	301.13	286.32	259.67	1.45	43.61	-8.45	2.50	5.38	0.11
1e	266.68	272.47	246.71	1.43	43.61	-8.25	2.64	4.37	0.18
1f	266.68	271.52	246.51	1.43	43.41	-8.64	2.81	1.53	-0.17
1g	250.23	261.68	237.79	1.41	42.99	-8.33	2.78	2.25	-0.06
1h	250.23	263.05	238.04	1.42	43.61	-8.17	2.70	3.80	0.45
1i	262.27	284.55	257.88	1.45	49.62	-7.75	3.30	2.26	0.56

MW: molecular weight (Da); MSA: molecular surface area (Å^2); MV: molecular volume (Å^3); Oval: ovality; PSA: polar surface area (Å^2); E_{HOMO}: energy of HOMO (eV); E_{LUMO}: energy of LUMO (eV), DM: dipole moment (Debye); C_{ele}: electrostatic charge of the C_4 carbon atom of the phenyl ring.

Taking into account the differences in the LUMO distribution and densities and the importance of the substituents at the *para* position of the phenyl ring, we calculated the electrostatic charge of carbon 4 (C_{ele}) (Table 2). Interestingly, we observed a strong correlation between the C_{ele} and the antiviral activity, since the most active derivatives exhibited the highest charges at this atom, except for compound **1a**.

Evaluation of the mechanism of action of the most active pyrazolone derivatives

We investigated the mechanism of action of the most active pyrazolone derivatives. First, we evaluated the direct effect of the compounds of the CHIKV particles. Interestingly, all compounds significantly inactivated virus particles and showed modest-to-strong virucidal effects, unlike CQ. For instance, compound **1i** decreased the virus titer by 55.64% whereas compounds **1a** and **1b** reduced 76.59% and 95.25% of CHIKV titer, respectively (Figure 3A). Then, we carried out a time-of-addition assay to analyze the inhibitory effects of the compounds at different steps of virus replication in Vero cells (Figure 3B). Compounds **1a** and **1i** showed the highest activity when added at -1 hpi and 0 hpi, respectively (42.67% and 50.16% inhibition), suggesting that these derivatives may act at the host-cell or early steps of virus replication in addition to the virucidal effect. Likewise, compound **1b** significantly impaired virus replication when added up to 4 hpi (>60% inhibition) which, in turn, indicated that this compound could act at different pre- and post-entry stages of the virus lifecycle.

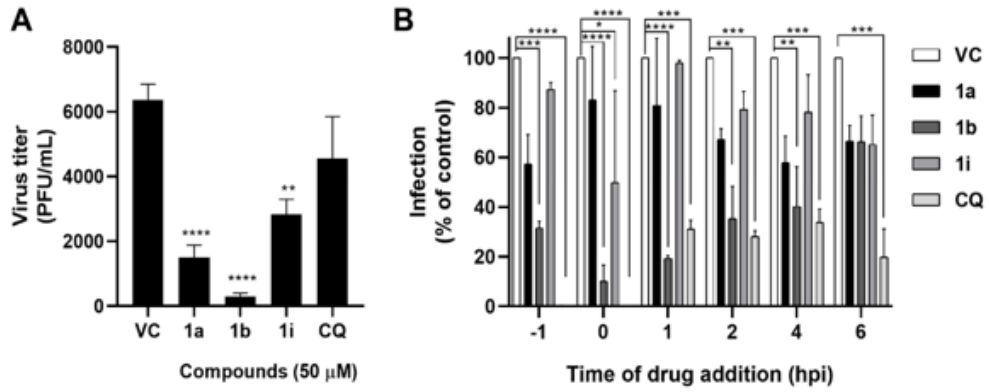

Figure 3: Mechanism of action analyses of the pyrazolone derivatives and the reference drug chloroquine (CQ) against CHIKV. (a) Virucidal activity. ~104 PFU of CHIKV were treated with 50 μM of the compounds for 2 h at 37 °C. After that, virus suspensions were diluted (1:50) and virus titers were quantified by plaque assays in Vero cells. (b) Time-of-addition assay. Compounds were added (300 μM) at different times during CHIKV infection (MOI 0.001), as follows: 1 h before infection (-1 hpi), during (0 hpi), or after infection (1, 2, 4, and 6 hpi). Compounds were kept for 1h and then discarded. At 7 hpi, cells were covered by overlay medium and incubated for 48 hrs at 37 °C for plaque assays. Data are expressed as mean ± standard deviation of, at least, two independent experiments measured in triplicate. Statistical significance was determined relative to the infected and untreated group (VC): *p<0.05, **p<0.01, ***p<0.001, ****p<0.0001.

Theoretical pharmacokinetic and toxicological profile of the most active compounds

To evaluate the drug-like profile of the pyrazolones, we predicted several pharmacokinetic and toxicological properties of the most active derivatives and compared them to CQ. The three pyrazolone derivatives **1a**, **1b**, and **1i** showed good human intestinal absorption (Table 3). In addition, they fulfilled the Lipinski "rule of five" requirements which indicate good oral bioavailability.

Table 3: In silico pharmacokinetic and toxicity properties of the pyrazolone derivatives and the marketed drug chloroquine (CQ).

Compounds	1a	1b	1i	CQ
Human Intestinal Absorption[a]	Yes (0.98)	Yes (0.98)	Yes (0.98)	Yes (1.00)
Ro5 violation	0	0	0	0
GSK 4/400	Approved	Approved	Approved	Approved
Pfizer 3/75	Warning	Warning	Warning	Rejected
Carcinogenicity[a]	No (0.64)	No (0.64)	No (0.74)	No (0.83)
Genotoxicity	No	Yes	Yes	No
Hepatotoxicity	No	No	No	Yes
Cardiotoxicity[b]	No	No	No	Yes
Irritant effects	No	Yes	No	Yes
Reproductive effects	No	No	No	No
Drug-likeness	-4.01	-3.82	-5.91	7.39
Drug-score	0.48	0.34	0.47	0.25

[a]Qualitative prediction results are presented along with the probability output in parenthesis. [b]Cardiotoxicity was predicted based on the inhibition of type I and II hERG potassium channels.

Besides, we applied other industry rules to evaluate the potential of these compounds (Table 3). GSK 4/400 rule states that compounds with MW > 400 Da and LogP > 4 have a greater probability to exhibit pharmacokinetic and toxicological issues [27]. All compounds were approved according to this rule, like CQ. On the other hand, Pfizer 3/75 rule defines that compounds with LogP > 3 and topological PSA (TPSA) < 75 $Å^2$ are more likely to show *in vivo* toxicity [28]. The three pyrazolone derivatives presented a warning alert due to their low TPSA (**1a** = 58.97 $Å^2$; **1b** = 58.97 $Å^2$; **1i** = 68.20 $Å^2$). It is worthy of note that the increased likelihood of having pre-clinical toxicity was observed for compounds that do not meet both criteria [28], such as observed for CQ. In addition to these rules, other toxicity risks were predicted for these compounds (Table 3). The pyrazolone derivatives did not present hepatotoxic, cardiotoxic, or reproductive toxic effects. However, the substituted derivatives **1b** and **1i** showed genotoxicity risk whereas the derivative **1b** exhibited irritant effects as well. Interestingly, these compounds hold a safer theoretical profile than the marketed drug CQ which was predicted to be hepatotoxic, cardiotoxic, and irritant. Furthermore, we calculated the drug-likeness and drug-score values of these compounds (Table 3). The drug-likeness refers to structural similarity with marketed drugs and non-drug-like compounds from the Fluka library. The three compounds showed low values in the range of -5.91 to -3.82 which indicates they have fragments that are mostly not found in the marketed drugs, such as the ethyl ester group. The drug-score combines several physicochemical and toxicological properties to infer the potential of the molecules as drug candidates. Despite the lower drug-likeness, all compounds showed higher drug-score values in comparison to CQ, especially the unsubstituted derivative **1a**, which, in turn, points to the promising drug-like profile of these compounds.

Discussion

Herein, we investigated the antiviral potential of pyrazolone derivatives against CHIKV replication in Vero cells. All the compounds analyzed have CC_{50} values in the range of 579 μM and 1,472 μM, proving their low cytotoxicity profile, even when compared to the marketed drug CQ (CC_{50} = 420 μM) selected as a positive control for *in vitro* anti-CHIKV assays as described elsewhere [22,29]. Consequently, the nine pyrazolone derivatives were screened for their inhibitory activity against CHIKV replication. At 50 μM, three compounds strongly reduced virus replication with inhibition rates of 68.15% for compound **1a**, 78.86% for compound **1b**, and 77.92% for compound **1i**. A more detailed analysis of the most active compounds was carried out to calculate their EC_{50} from dose-response curves. The unsubstituted pyrazolone **1a** presented an EC_{50} of 34.67 μM while compound **1b**, which has 2,4-dichloro groups, showed the highest activity (EC_{50} = 26.44 μM).

SAR studies were then performed to gain more insights into the anti-CHIKV properties of these derivatives. We observed that the introduction of electron-withdrawing groups, such as halogens, at *para* and *ortho* positions simultaneously of the phenyl ring favored the antiviral activity. Interestingly, the introduction of halogens in the phenyl ring of scaffolds bearing a pyrazolone moiety improved the antiviral properties against the replication of RNA viruses such as Coxsackie viruses A and B [30] as well as against the main protease (Mpro) activity of SARS-CoV[31]. In contrast, the presence of an electron-donating group (*e.g.*, methoxy) at the *para* position of the same ring improved the activity as well. Further structural modifications are of great interest to better address the SAR of these compounds.

We also investigated the stereo electronic features to correlate to their biological activity. A direct correlation between PSA, $E_{HOMO,}$ and E_{LUMO} and their inhibitory activity was noticed. In general, the frontiers orbitals are involved in the ligand-receptor interactions and the higher density and distribution of LUMO orbitals over the phenyl ring likely contribute to their antiviral profile. Also, the nature and position of the substituents of the phenyl ring influence the electrostatic charge of carbon 4 of the phenyl ring (C_{ele}), and our results indicate that this influence is important to the maintenance of their anti-CHIKV activity.

Although the pyrazolone derivatives were not as active as the control CQ, both compounds **1a** and **1b** had higher selectivity. Despite the lower cell selectivity of compound **1i** in comparison to the control drug, this compound still offers an interesting safety window because its CC_{50} value is nearly 21-fold higher than its EC_{50}. Hence, considering the promising potential of these derivatives, we investigated the mechanism of action of the most active compounds. Initially, we evaluated whether these compounds could inactivate directly the CHIKV particles. All compounds exhibited virucidal activity and significantly reduced virus titers. Interestingly, *in silico* studies have suggested that other pyrazolone derivatives could interact with surface-exposed proteins (*e.g.*, spike proteins) of the RNA virus SARS-CoV-2 and exert virucidal activity. Also, these derivatives were shown to interact with other targets, such as papain-like and main proteases, and inhibit virus replication [32].

We further evaluated at which steps of virus replication the compounds could act by adding them at different times of infection. The three compounds presented significant inhibitory activity at the first times of time-of-addition assays, indicating they act at early stages like virus attachment or entry. Similarly, Oliveira and coworkers [33] demonstrated that the organometallic complex [Ru-2Cl4(p-cymene)2] inhibited the early steps of the CHIKV virus due to its virucidal activity triggered by an interaction with the viral envelope proteins. The same was observed for one phospholipase A2 isolated from the snake venom of *Crotalus durissus terrificus* [34]. The virucidal activity of the pyrazolone derivatives may contribute to their activity at the early stages of the virus life cycle. Besides, compound **1b** presented more prominent activity when added until 4 hpi, suggesting that it acts at other post-entry steps that are still to be assessed. In fact, different compounds have multiple mechanisms of action against CHIKV, such as the natural products baicalin [35] and harringtonine[36], and the synthetic benzimidazole MB-ZM-N-IBT [37], which is interesting to curtail resistance emergence and spread.

In the drug development process, undesirable pharmacokinetic and toxicological properties are one of the leading causes of drug failure [38]; thereby, we predicted some ADMET properties of the most active compounds. The three derivatives have high human intestinal absorption and good oral bioavailability according to Lip-

inski's "rule of five", pointing them as suitable for oral delivery. Also, they were approved in GSK 4/400 rule, but a warning was raised regarding the Pfizer 3/75 one, unlike CQ which was rejected.

Moreover, we analyzed some theoretical toxic properties, and the three derivatives exhibited a safer profile than the marketed drug CQ. The higher drug-score values of these compounds in comparison to CQ, especially the unsubstituted derivative **1a**, highlight their potential as drug candidates and encourage further hit-to-lead optimization campaigns to improve their anti-CHIKV activity. Finally, it is important to note that the studied compounds share a common scaffold with the anti-inflammatory drug antipyrine and its derivatives which possess antiviral activity against RNA viruses [30]. Therefore, in addition to the antiviral activity, the compounds selected in our work may be endowed with anti-inflammatory properties which are highly desired to treat CHIKV infections, but it remains to be explored in the future.

Conclusion

In the present study, we have identified three pyrazolone derivatives (**1a**, **1b**, and **1i**) with significant *in vitro* antiviral activity against CHIKV and good selectivity. Their activity is likely modulated by parameters such as PSA, E_{HOMO}, $E_{LUMO,}$ and LUMO distribution as well as the electrostatic charge of the carbon 4 of the phenyl ring. Further, the mechanism of action evaluation showed that these compounds act at early steps of virus replication in addition to their high virucidal activity. Also, compound **1b** significantly inhibited virus replication at post-entry steps, pointing to multiple mechanisms of action. Finally, the pharmacokinetic and toxicological predictions reinforced the promising potential of these compounds as drug candidates which deserve further investigations to fight CHIKV infections.

Acknowledgement

This study was financed in part by the Coordenação de Aperfeiçoamento de Pessoal de Nível Superior – Brasil (CAPES) – Finance Code 001. In addition, this work was supported by Brazilian agencies National Council for Scientific and Technological Development (CNPQ) and Research Support Foundation of the State of Rio de Janeiro (FAPERJ).

Conflict of Interest

The authors declare no competing financial interest.

References

1. Javaid A, Ijaz A, Ashfaq UA, Arshad M, Irshad S, et al. (2022) An overview of chikungunya virus molecular biology, epidemiology, pathogenesis, treatment and prevention strategies. Future Virol 17: 593-606.
2. Teng T-S, Kam Y-W, Tan JJL, Ng LFP (2011) Host response to Chikungunya virus and perspectives for immune-based therapies. Future Virol 6: 975-984.
3. Tozan Y, Sjödin H, Muñoz ÁG, Rocklöv J (2020) Transmission dynamics of dengue and chikungunya in a changing climate: do we understand the eco-evolutionary response? Expert Rev Anti Infect Ther 18(12): 1187-1193.
4. Kumar R, Ahmed S, Parray HA, Das S (2021) Chikungunya and arthritis: An overview. Travel Med Infect Dis 44: 102168.
5. Ghildiyal R, Gabrani R (2020) Antiviral therapeutics for chikungunya virus. Expert Opin Ther Pat 30(6): 467-480.
6. Wang P, Zhang R (2019) Chikungunya Virus and (Re-) Emerging Alphaviruses. Viruses 11(9): 779.
7. ECDC (2023) Chikungunya worldwide overview. Accessed.
8. Secretaria de Vigilância em Saúde e Ambiente (2023) Monitoramento dos casos de arboviroses até a semana epidemiológica 52 de 2022. Ministério da Saúde - Bol Epidemiológico 54: 1-14
9. Casulli A (2021) New global targets for NTDs in the WHO roadmap 2021–2030. PLoS Negl Trop Dis 15(5): e0009373.
10. Khongwichit S, Chansaenroj J, Chirathaworn C, Poovorawan Y (2021) Chikungunya virus infection: molecular biology, clinical characteristics, and epidemiology in Asian countries. J Biomed Sci 28(1): 84.
11. Amaral JK, Bilsborrow JB, Schoen RT (2020) Chronic Chikungunya Arthritis and Rheumatoid Arthritis: What They Have in Common. Am J Med 133(3): e91-e97.
12. Cavalcanti TYV de L, Pereira MR, Paula SO de, Franca RF de O (2022) A Review on Chikungunya Virus Epidemiology, Pathogenesis and Current Vaccine Development. Viruses 14(5): 969.
13. Sharma R, Chawla PA, Chawla V, Verma R, Nawal N, et al. (2021) A Therapeutic Journey of 5-Pyrazolones as a Versatile Scaffold: A Review. Mini Rev Med Chem 21(13): 1770-1795.
14. Asif M, Imran M, Husain A, Asif M, Imran M, et al. (2021) Approaches for chemical synthesis and diverse pharmacological significance of pyrazolone derivatives: a review. J Chil Chem Soc 66: 5149-5163.
15. Mustafa G, Zia-ur-Rehman M, Sumrra SH, Ashfaq M, Zafar W, et al. (2022) A critical review on recent trends on pharmacological applications of pyrazolone endowed derivatives. J Mol Struct 1262: 133044.
16. Zhao Z, Dai X, Li C, Wang X, Tian J, et al. (2020) Pyrazolone structural motif in medicinal chemistry: Retrospect and prospect. Eur J Med Chem 186: 111893.
17. Faria JV, Vegi PF, Miguita AGC, dos Santos MS, Boechat N, et al. (2017) Recently reported biological activities of pyrazole compounds. Bioorg Med Chem 25(21): 5891-5903.
18. Cirne-Santos CC, Barros C de S, Nogueira CCR, Azevedo RC, Yamamoto KA, et al. (2019) Inhibition by marine algae of chikungunya virus isolated from patients in a recent disease outbreak in rio de janeiro. Front Microbiol 10: 2426.
19. Desimoni G, Righetti PP, Selva E, Tacconi G, Riganti V, et al. (1977) Heterodiene syntheses—XIX: Correlation of the kinetic data with lumo energies in the reaction between 1-aryl-4-benzylidene-5-pyrazolones and isopropyl vinyl ether. Tetrahedron 33(21): 2829-2836.
20. Newman GA, Pauwels PJS (1969) A study of pyrazolin-5-one tautomerism—I : Some 3-unsubstituted 1-aryl-2-pyrazolin-5-ones. Tetrahedron 25(18): 4605-4615.
21. Das N, Verma A, Shrivastava PK, Shrivastava SK (2008) Synthesis and biological evaluation of some new aryl pyrazol-3-one derivatives as potential hypoglycemic agents. Indian J Chem 47B:1555-1558.
22. Khan M, Santhosh SR, Tiwari M, Lakshmana Rao PV, Parida M (2010) Assessment of in vitro prophylactic and therapeutic efficacy of chloroquine against Chikungunya virus in Vero cells. J Med Virol 82: 817-824.
23. Daelemans D, Pauwels R, De Clercq E, Pannecouque C (2011) A time-of-drug addiction approach to target identification of antiviral compounds. Nat Protoc 6(6): 925-933.
24. Yang H, Lou C, Sun L, Li J, Cai Y, et al. (2019) admetSAR 2.0: web-service for prediction and optimization of chemical ADMET properties. Bioinformatics 35(6): 1067–1069.
25. Pires DE V, Blundell TL, Ascher DB (2015) pkCSM: Predicting Small-Molecule Pharmacokinetic and Toxicity Properties Using Graph-Based Signatures. J Med Chem 58: 4066-4072.

26. Lagorce D, Bouslama L, Becot J, Miteva MA, Villoutreix BO (2017) FAF-Drugs4: free ADME-tox filtering computations for chemical biology and early stages drug discovery. Bioinformatics 33: 3658-3660.

27. Gleeson MP (2008) Generation of a set of simple, interpretable ADMET rules of thumb. J Med Chem 51(4): 817-834.

28. Hughes JD, Blagg J, Price DA, Bailey S, DeCrescenzo GA, et al. (2008) Physiochemical drug properties associated with in vivo toxicological outcomes. Bioorganic Med Chem Lett 18: 4872-4875.

29. Bassetto M, De Burghgraeve T, Delang L, Massarotti A, Coluccia A, et al. (2013) Computer-aided identification, design and synthesis of a novel series of compounds with selective antiviral activity against chikungunya virus. Antiviral Res 98: 12-18.

30. Evstropov AN, Yavorovskaya VE, Vorob'ev ES, Khudonogova ZP, Gritsenko LN, et al. (1992) Synthesis and antiviral activity of antipyrine derivatives. Pharm Chem J 26: 426-430.

31. Ramajayam R, Tan KP, Liu HG, Liang PH (2010) Synthesis and evaluation of pyrazolone compounds as SARS-coronavirus 3C-like protease inhibitors. Bioorg Med Chem 18: 7849-7854.

32. Branković J, Milovanović VM, Simijonović D, Novaković S, Petrović ZD, et al. (2022) Pyrazolone-type compounds: synthesis and in silico assessment of antiviral potential against key viral proteins of SARS-CoV-2. RSC Adv 12: 16054-16070.

33. Oliveira DM de, Santos I de A, Martins DOS, Gonçalves YG, Cardoso-Sousa L, et al. (2020) Organometallic Complex Strongly Impairs Chikungunya Virus Entry to the Host Cells. Front Microbiol 11: 608924.

34. Santos IA, Shimizu JF, de Oliveira DM, Martins DOS, Cardoso-Sousa L, et al. (2021) Chikungunya virus entry is strongly inhibited by phospholipase A2 isolated from the venom of Crotalus durissus terrificus. Sci Reports 11(1):8717.

35. Oo A, Rausalu K, Merits A, Higgs S, Vanlandingham D, Bakar SA, et al. (2018) Deciphering the potential of baicalin as an antiviral agent for Chikungunya virus infection. Antiviral Res 150: 101-111.

36. Kaur P, Thiruchelvan M, Lee RCH, Chen H, Chen KC, et al. (2013) Inhibition of Chikungunya virus replication by harringtonine, a novel antiviral that suppresses viral protein expression. Antimicrob Agents Chemother 57(1): 155-167.

37. Mishra P, Kumar A, Mamidi P, Kumar S, Basantray I, et al. (2016) Inhibition of Chikungunya Virus Replication by 1-[(2-Methylbenzimidazol-1-yl) Methyl]-2-Oxo-Indolin-3-ylidene] Amino] Thiourea (MBZM-N-IBT). Sci Rep 6: 1-13.

38. Wu F, Zhou Y, Li L, Shen X, Chen G, et al. (2020) Computational Approaches in Preclinical Studies on Drug Discovery and Development. Front Chem 8: 726.